Influence of friction stir processing rotational speed on microstructure and mechanical properties of AA2024 nanocomposite

Wael Hoziefa [a], Amir A. Mahdy [a], M.M.Z. Ahmed [b], I. El-Mahallawi [c], A. Atlam [a]

(a) Department of Metallurgy, Mining & Petroleum Engineering, Faculty of Engineering, Al-Azhar University, Egypt.
(b) Department of Metallurgical and Materials Engineering, Faculty of Petroleum and Mining Engineering, Suez University, Egypt.
(c) Department of Metallurgy and Materials Engineering, Faculty of Engineering, Cairo University, Egypt

Abstract— Compocasting technique was used to produce AA2024 / Al_2O_3 nano composite materials. Aiming to evaluate the effect of friction stir processing (FSP) rotational speed on nanoparticles distribution and mechanical properties of the composite, AA2024/Al_2O_3 plates were subjected to friction stir processing at different rotation speeds of 400, 600, 800 and 1000 rpm. For comparison, plates of AA2024 were similarly produced. Light Optical Microscopy (LOM) and Scanning Electron Microscopy (SEM) were used to examine casted and the friction stir processed (FSPed) materals. Tensile and hardness testing were carried out for both materials. A non-uniform distribution and particle clustering of Al_2O_3 particulates were observed in composite. Some porosity and voids due to casting process were also detected. The use of FSP greatly enhanced the distribution of the nano Al_2O_3 particles and significantly refined the grain structure of the AA2024 matrix. As a result, the ultimate strength of the FSPed material increased to about four times (from 72 MPa for the as cast to 316 MPa after FSP) and the hardness almost doubled (from 93 Hv for the as cast to about 155 Hv after FSP).

Index Terms—Nanocomposite MMCs, compocasting technique, Al_2O_3 nano particles, friction stir processing (FSP).

1 INTRODUCTION

Compocasting route is a rheocasting process that involves the injection of reinforcement particles into semisolid state alloys. Compocasting is generally thought to be a processing route allowing to obtain quite uniform distribution of reinforcing particles, as well as to enhance particle wettability [1].

Despite these advantages, some agglomerates, inevitably induced by the high surface-to-volume ratio, as well as to Van der Waals interactions are still reported [2].

Mazaheryet al. [3] shows that it is extremely difficult for the mechanical stirring method to distribute and disperse nano-scale particles uniformly in metal melts due to their large surface-to volume ratio and their low wettability in metal melts, which easily induce agglomeration and clustering.

El-Mahallawi et al. [4-5] studied the influence of nanodispersions on mechanical properties of semisolid Al casts using nanoparticles as reinforcement agents, results showed enhancement in the tensile strength reached to about 195 MPa of the Al_2O_3 nano-dispersed alloys, accompanied by significant increase in the elongation percentage, supported by evidence of refined structure.

The effect of heat treating Al_2O_3 nanoparticles prior to its addition into molten Al matrix was studied by Zadeh et al. [6]. The heat treatment improved the wettability due to grooving at the grain boundary junctions, thereby improving the microstructure and mechanical properties when compared to the nanocomposite having particles without any heat treatment.

The production of Al 2024 reinforced with 1% wt. nano Al_2O_3 particulates was produced using mechanical stir casting process with assistance of argon gas [7], the results show that the fabrication of metal matrix nano composites (MMNCs) using mechanical stir casting process generally results poor distribution of nano particles within the matrix and had bad effect on the ultimate tensile strength and yield strength.

Rahimi et al. [8] reported the effects of stirring speed on the microstructure and mechanical properties of Al-2024 alloy synthesized by a rheocasting process. A decrease in grain size of

α-Al particles corresponding to an increase in stirring speed was recorded. It was also found that the hardness, compressive strength, and compressive strain increased with the increase of stirring speed. Microstructural studies revealed the presence of nonsoluble Al_{15} $(CuFeMn)_3$ Si_2 phase in the vicinity of $CuAl_2$ in the rheocast samples.

Marini et al. [9] reported that the synthesis of MMNCs by conventional casting method has shown a limitation due to low wettability of the reinforcement phase by the molten metal, and the best techniques to fabricate the aluminum matrix nanocomposite (Al-MNCs) is powder metallurgy (PM), for its mass production and cost effectiveness.

Friction stir processing (FSP) is unique solid state technique used for microstructure modification and grain refining [10]. FSP was used for microstructure modification of cast aluminum alloys to enhance theirmechanical properties [11-13].

Karthikeyan et al. [14] studied the effects of FSP on microstructure and mechanical properties of cast aluminum alloy of 2285 grade. Results show improved mechanical properties have been observed for all parameters. Mahmoud et al. [15] used FSP in improvement of microstructural, mechanical characteristics of A413 cast Al Alloys, results show that FSP has significantly improved microstructure of A413 alloy by eliminating structural defects such as porosity and Si segregation, also size of alpha-Al grains increases with increase of rotational speed. Wais et al. [16] studied the effect of FSP parameters such as transverse speed (86,189,393mm/min), rotational speed (560,710, 900rpm) on microstructure and mechanical properties of sand casting hypereutectic pure Al using a cylindrical tool with threaded pin. After FSP, the microstructure of the cast pure Al was greatly refined. However, FSP caused very little changes to the hardness of the material, while tensile and impact properties were greatly improved.

Also FSPof alumina particle reinforced aluminum alloys has also been studied [17, 18]. Ahmed, et al. [19, 20] developed AA7075/nano-alumina composite using FSP; the results showed that FSP can be utilized to develop surface-nanocomposites with Al_2O_3 nanodispersions embedded in the matrix. The new surface nanocomposites showed enhancement in the hardness of the surface of A7075 to almost double of the starting material. The stirring of the FSP tool has a substantial influence on the distribution of alumina particles in Al_2O_3/Al composites [21]. Cavaliere et al. [22] show that the stirring of the tool can also change the shape of the reinforcement particles. It breaks off the sharp edges of the bigger particles, rounding them up at the same time, this action results in smaller, round particles in the nugget. The current study utilizes the reho-casting and FSP in the development of nanocomposite through the investigation of FSP rotation speed effects on the microstructure and mechanical properties of reho-cast Al 2024/ Al_2O_3 nanocomposite.

2 MATERIALS AND METHOD

A commercial wrought-grade aluminum alloy (AA 2024) with the chemical composition shown in Table 1, was used as the metallic matrix material.

Nano Al_2O_3 particulates with average particle size of 50 nm shown in Fig.1 were used as the reinforcement materials.

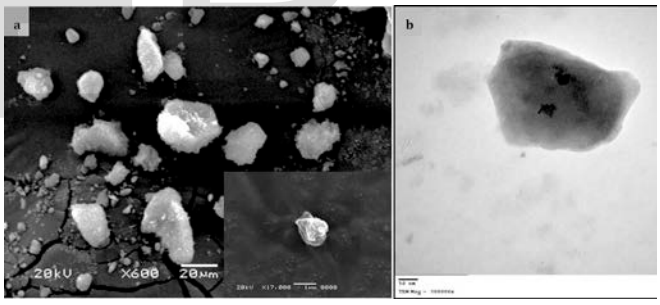

Fig.1 SEM micrograph shows aglometarted Al_2O_3 particle (a), and TEM shows single nano Al_2O_3 particle (b)

A charge of 400 gm of the Al base alloy was melted in an electric heat resistance furnace, using a carbide crucible, and a three blade graphite stirrer driven by speed motor of 900-1200 rpm, which was used for stirring. After reaching the liquid state the melt was degassed with hexachlorethane degasser tablets, to get rid of gases. The temperature was then lowered gradually until the alloy matrix reached a semi-solid state. At this temperature

(630ºC) the reinforcing Al_2O_3 particles were introduced into the slurry. The high viscosity of the slurry combined with the action of stirring helps in minimizing the tendency for floating, settling, or agglomeration of Al_2O_3 particles. The nano Al_2O_3 particles were previously treated using high energy ball mill for about 5 minutes in order to avoid particle clustering, then packaged in aluminum foil (1% of charge weight). The packages were preheated for 3 hour at 200° C before being introduced to the molten aluminum alloy.The slurrywas cast in a stainless steel mould with dimensions of 250 mm length, 50 mm width and 10 mm thickness.

The FSW/FSP machine was used for processing of the as cast materials at different rotation rates. The process was carried out using a cylindrical FSP tool made of H13 tool steel heat-treated to obtain 58 HRC hardness. The FSP tool dimensions were 6 mm probe diameter, 6 mm probe length and 20 mm diameter shoulder. FSP was performed at rotation speeds of 400, 600, 800 and 1000 rpm, traverse speed of 20 mm/min, and tool the tilt angle was set at 3º.

Macrographs of the cross sections of the as-cast and FSP samples were obtained through a multifocal microscope (Hirox). In order to carry out microstructural analyses of the unreinforced matrix and nanocomposite, in the as-cast condition and after FSP, metallographic samples were prepared for examination by using light optical microscopy (LOM) and scanning electron microscopyequipped with energy dispersive spectroscopy (SEM EDS). Representative sections were cut from the cross-section of cast and FSP plates, then wet grounded using silicon carbide abrasive discs of increasing fineness (from 120 to 4000 grit) and finally polished using 3 μm and 1 μm diamond paste. Samples for LOM and SEM analyses were etched with Keller's reagent.

Mechanical properties of the investigated materials were measured at ambient temperature by tensile tests and Vickers microhardness profiles. Rounded tensile specimens (according to ASTM B557M) were cut along cast and FSPed plate, aiming to have the entire gauge section in the FSP zone, samples were cut in FSP zone . Three tensile specimens for each material, both in the as-cast and after FSP, were tested using an electromechanical testing machine.

Vickers microhardness measurements were performed on the cross section of the FSP samples, under 4.9 N load andfor a dwell time of 10s. 20 microhardness indentations were performed every 500 μm at different depth of 0.5 mm, 2.5 mm and 4.5 mm from surface for either cast or friction stir processed (FSPed) samples as shown in Fig.2.

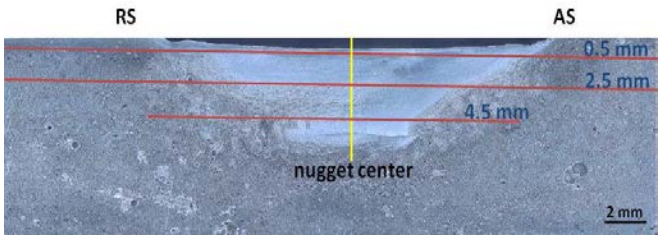

Fig.2 Microhardness readings procedure from processed surface

3. Results and Discussion

3.1 Microstructural analyses

The optical macrographs of the unreinforced and reinforced as cast materials before applying FSP are shown in Figure 3. It can be seen that the cross section of the as cast AA2024 (Fig.3a) is clear with no obvious defects noticed, while, clusters and cavities can be seen in the as cast AA2024/Al_2O_3 nano dispersed samples (Fig.3b). The presence of pores in the semi-solid processed composite was expected, as widely reported by several investigators [2-8], this is due to the effect of low wettability and agglomeration at high content of reinforcement and pore nucleation at the matrix–Al interfaces. Moreover, decreasing liquid metal flow associated with the particle clusters leads to the formation of porosity. It was reviewed that porosity levels should be kept to minimum as this kind of a composite defect can be detrimental to the corrosion resistance of the casting and it can control mechanical properties of the cast metal. It arises due to gas entrapment, during mixing, hydrogen evolution and shrinkage, wettability issue between reinforcement and matrix alloy increasing tendency for agglomeration of particles [26].

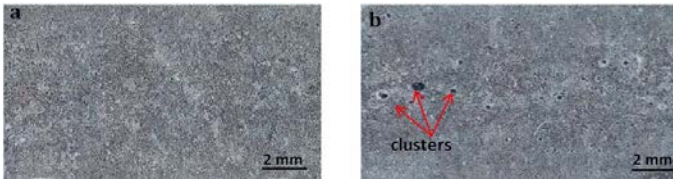

Fig.3 Macrograph of rheocast AA2024 without additions (a), and AA2024 reinforced with 50 nm Al_2O_3 particles (b)

Figure 4 shows typical microstructure nano composite samples obtained using rheocasting technique. The conventional cast microstructure shows primary α (Al) dendrites surrounded by the eutectic structure, with the intermetallic compounds consisting of Al_2Cu and Al_2CuMg. However the structure changed after mechanical stirring and nanoparticles addition to be spherdiozed, with some regions still showing dendritic structure.

The α-dendrites are characterized by a quasi-globular morphology, more accentuated in the composite. Similar behavior has been reported, supporting that the addition of Al_2O_3 nano-particles to aluminum alloys has reduced the grain size of the aluminum matrix [5-6, 13]. It is also worth mentioning that the as-cast microstructure shows manycavities and pores in the as cast samples.

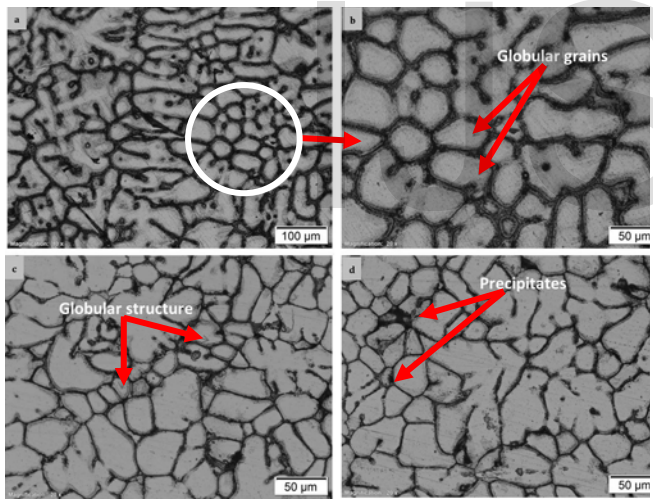

Fig.4 Optical micrographs of semisolid dendrite structure of unreinforced matrix AA2024 (a, b), and semisolid globular structure of AA2024 reinforced with Al_2O_3 (c, d), at different magnification

Figure 5 shows typical SEM micrographs of the as cast AA2024 sample, the dendrite structure surrounded by a nonequilibrium eutectic phase. Composition of intermetallic particles was investigated through EDS analyses from the two observed regions are depicted in Fig.5, revealing the presence of small particles containing Al, Cu and Mg (probably the Al_2Cu and Al_2CuMg phases) in the interdendritic regions. A presence of these phases was reported [11], because of low solubility of iron in aluminum, these elements combine with other alloying elements (Cu, Mn, and Si) segregated due to the applied shear stress. This leads to the formation of a nonsoluble phase (Al_{15} (CuFeMn) $_3$ Si_2) in the vicinity of the $CuAl_2$ phase at the grain boundaries of the cast sample.

SEM analyses carried out on the nanocomposite confirmed the relationship between porosities and nanoparticles as shown in Fig.6. Internal surfaces of pores, in fact, showed the presence of alumina clusters, which probably induced their formation. The particles clustering in the voids observed in the macrostructure of AA2024/ Al_2O_3 nanocomposite samples were analyzed, as shown in Fig. 6 (d, f). The morphology of the alumina was identified in the form of clusters. Extended analysis shows that the alumina clusters are not only found in pores but also within the dendrite arms. These clusters were reported to cause the low yield strength, which restricts the nanocomposites industrial applications [5-8].This shows that the main aim of mechanical properties improvement, targeted by composite reinforcement with nanoparticles, is hindered by the nanoparticles clustering. Clustering of the nanoparticles at the cavities and pores, which are the last parts to solidify, has been explained by the tendency of these alloys to exhibit a pushing mechanism for the foreign particles, rather than the engulfment mechanisms shown when the particles are homogeneously incorporated within the grain boundaries during solidification.

It has been shown that as the slurry of the melt contains more liquid phasesremaining and when the heat extraction by the die is non-uniform, some irregular particles are produced at the cavities as shown in the microstructure in Fig.6 [8].

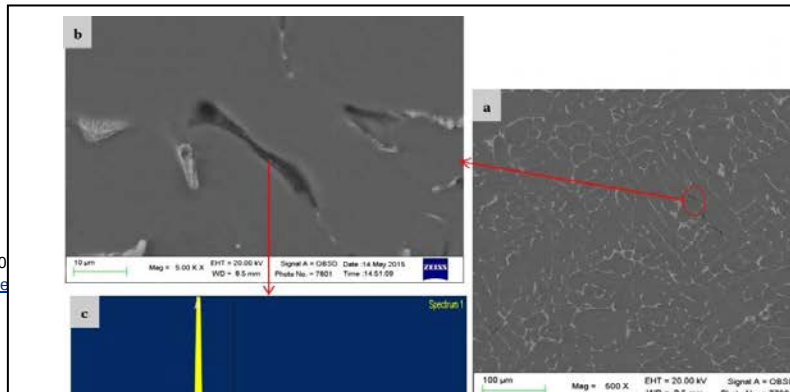

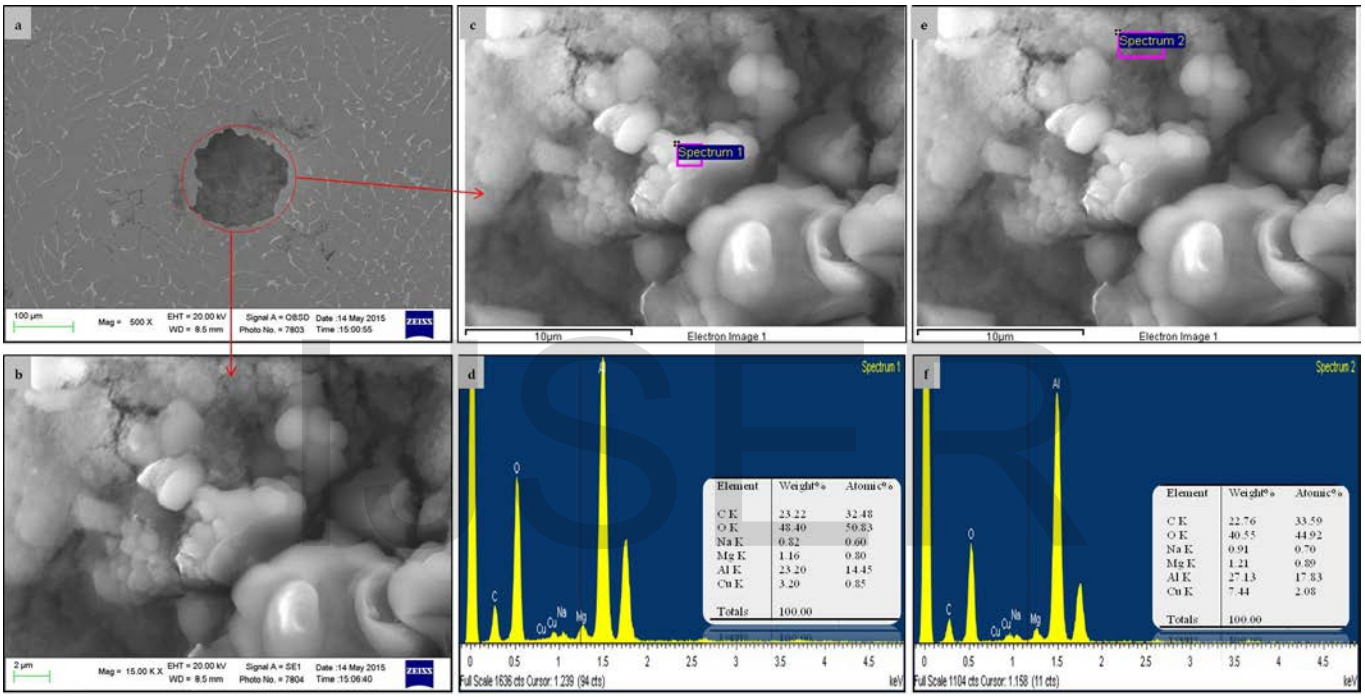

Fig.6 SEM micrograph of rheocast AA 2024/ Al_2O_3 (a), shows presence of internal porosity associated with nanoparticles clusters found at the pore boundaries (b, c, e) with associated EDS spectrum (d,f).

3.2 MICROSTRUCTURE OF FSPED MATERIALS

The experiments discussed and mainly concentrate on the FSP rotational speed effect on the AA 2024 cast alloy, with a view to first providing an overview of the general effects observed in FSP, before focusing in more depth on specific areas of interest. In general, the microstructure of the cast AA 2024 alloys was found to be greatly refined by FSP, as has been reported previously by other authors [14, 15].

Optical macrographs of transverse cross sections of the FSPed materials, processed at a transverse speedof 20 mm/ min and a rotation rate of 400, 600,800 and 1000 rpm, are shown in Fig.7, the region indicating the nugget zone (NG) taken from the as-cast material are shown and compared to that of the advancing and retreating side of the NG at the mid-plane.

It can be observed that the NG zone in the reinforced material have sharper edges and is more homogenous in terms of brightness especially at 400 and 1000 rpm. Another important feature to be noted in the FSPed zone of the reinforced material is the disappearance of the clusters and voids observed in the as cast material.

As rotational speed increased during FSP, the casting defects like porosity, cracks, blow holes, etc., were eliminated due to frictional heat generated between the tool and the material, coupled to the stirring action of the tool pin which leads to material flow. Also no defects such as piping defects, tunnel defects, pin holes, kissing bond that could persist in the FSP/FSW material due to insufficient heat input or inadequate/ improper plastic flow [17] can be observed. This implies that the FSP parameters used resulted in sufficient heat input and proper material flow for producing sound stir zone.

It can be observed that the size of the processed zone is decreasing by increasing the rotation speed with the max size at 400 rpm as it can be noted from the super imposed NG size at 400 rpm on the macrographs in Fig.7. This can be attributed to the change in the contact condition of the FSP tool with the surrounding material from sticking condition at low rotation speed to slipping condition at high rotation speeddue to the increase of the heat input [24].

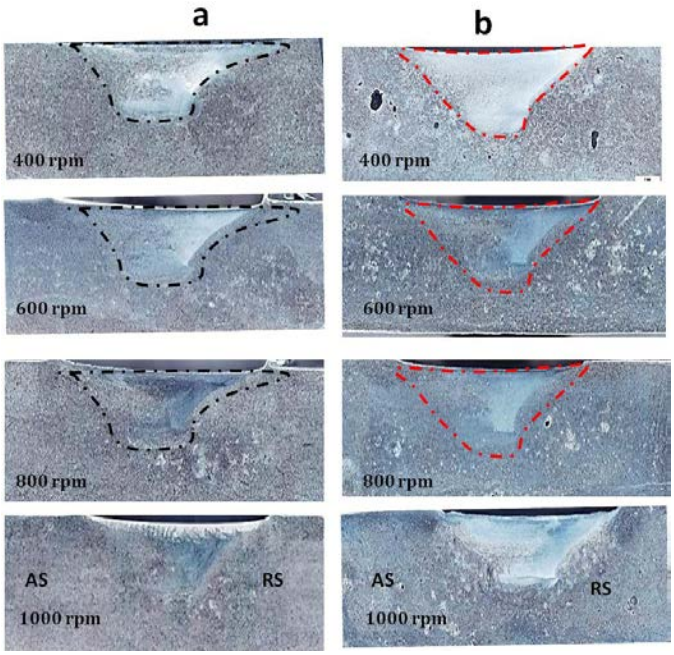

Fig.7 Nugget size and shape macrostructure at rotation rate of 400,600,800 and 1000 rpm for the processed as cast AA2024 (a), and AA2024 reinforced with Al_2O_3 nano particles (b). Dashed lines represent the size of the NG at 400 rpm

Optical microscopy examination was carried out to study the influence of the rotational speed on the microstructure of FSPed region. Optical microscopy micrographs obtained at the same magnification from the stir zone of the as cast compared to that of nano-reinforced samples which FSPed at different rotation rates; i.e. 400 rpm as shown in Fig.8 and 800 rpm as shown in Fig.9. As it can be seen from the figures, a significant grain size reduction in the stir zone has occurred relative to the cast material grain structure. In addition, the nano particles cluster size is reduced and the reinforcement distribution is improved.

Breaking the intermetallicsformed at casting and further separation of particlesfrom the clusters during FSP resulted in improved nanoparticle distributions. As rotational speed increased, the structure of the nugget zone is to be fine, and the cluster size of alumina nanoparticles increased due to increase in heat input and material flow in the stir zone. These results are revealed in particle size examinations as can be seen in these figures, although in all conditions, clustering occurred, but the percent of large clusters is low at 400 rpm in comparison to 800 rpm for nanoreinforced samples.

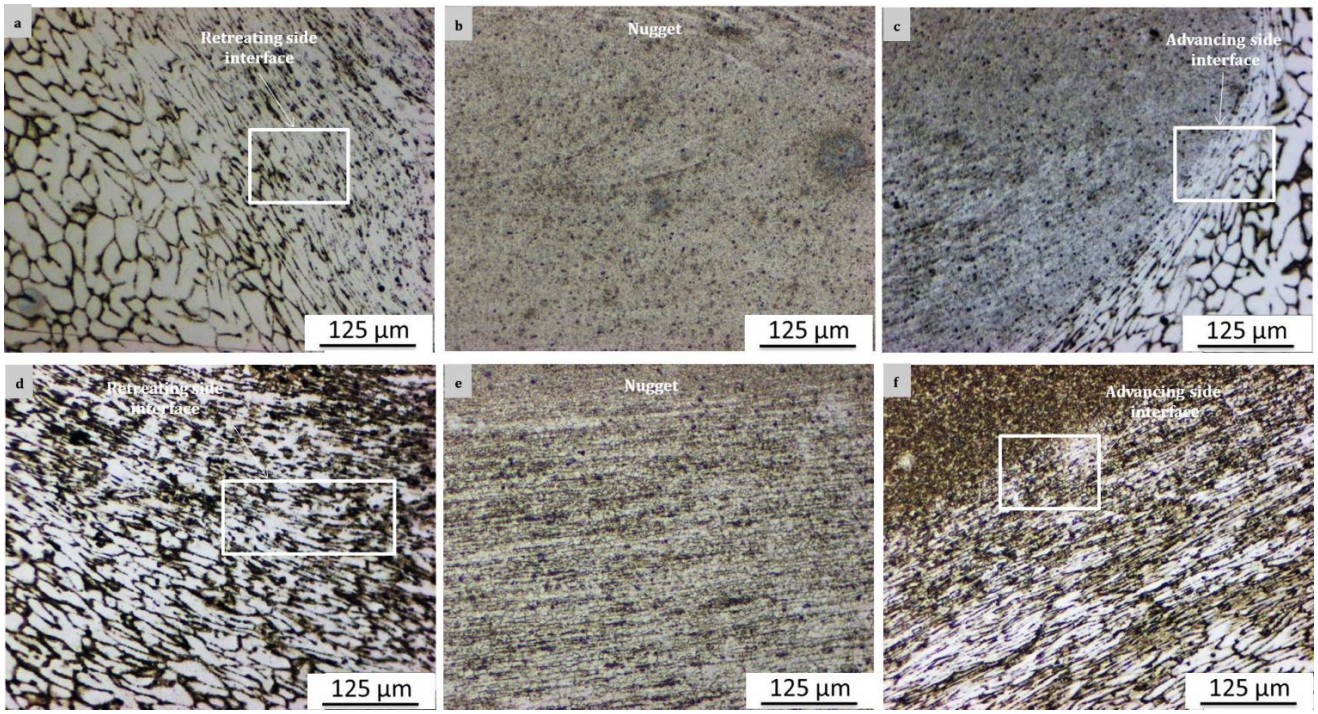

Fig.8 Optical micrographs of FSPd AA 2024 zones from (a) retreating side (RS) ,(b) process zone (PZ) and (c) advancing side (AS) and FSPd AA 2024/ Al_2O_3 (d ,e ,f) respectively at rotation rate of 400 rpm

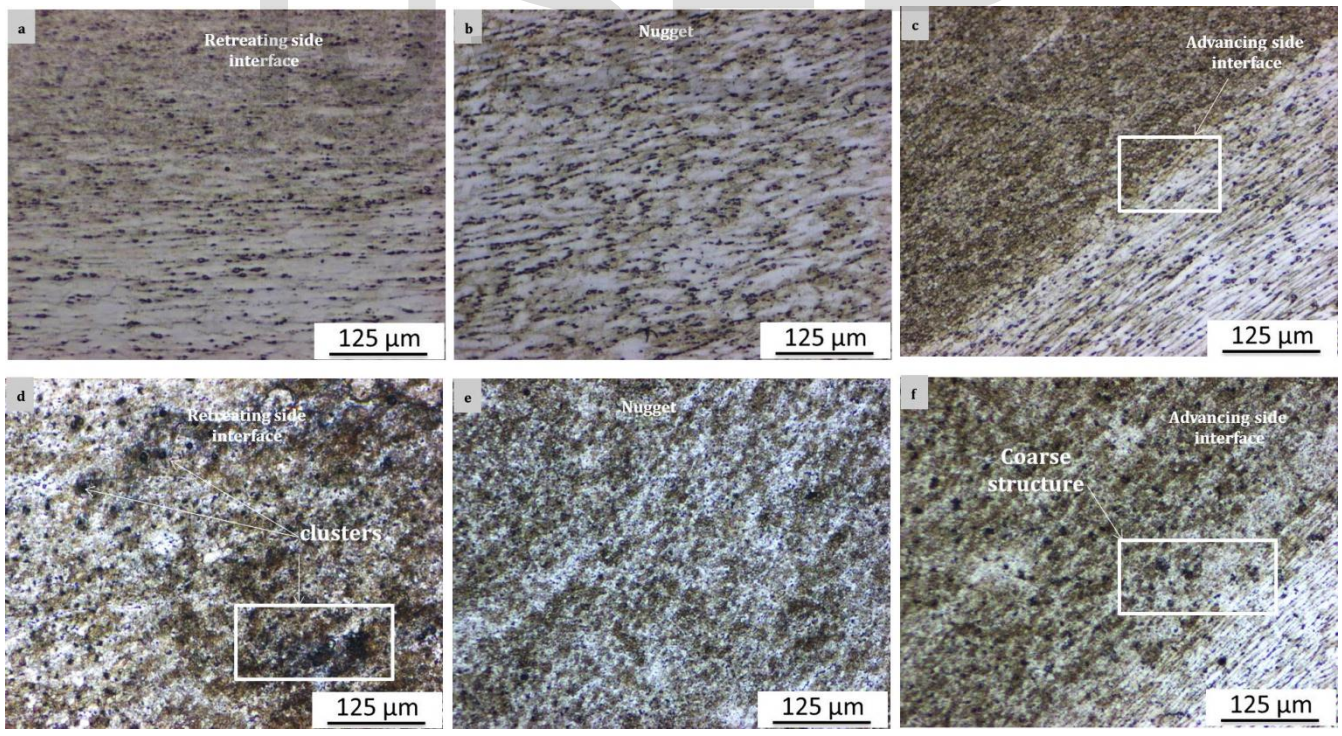

Fig.9 Optical micrographs of FSPed AA 2024 zones from (a) retreating side (RS) , (b) process zone (PZ) and (c) advancing side (AS) and FSPd AA 2024/ Al_2O_3 (d ,e ,f) respectively at rotation rate of 600 rpm

The microstructural results using Scanning Electron Microscope (SEM) accompanied with Energy- Dispersive Spectroscopy (EDS) of the base matrix AA 2024 and the AA 2024/ Al_2O_3 at different rotation rates of 400, 600, 800 and 1000 rpm are shown in Figures (10-13).

Figure 10 shows the grain structure of the as-cast material and FSPed samples at 400 rpm rotational speed, the dendritic structure of as cast AA2024 was greatly refined after FSP; however, the grain structure is clearly more equiaxed and more homonized, microstructural homogeneity was necessarily achieved throughout the processed zone as shown in Fig.10 (a). Comparative SEM micrographsat same magnifications for AA 2024 at base materialand NG zone is also shown in Figure 10 (a, b). EDS of the processed specimens showed areduction in the percentage of elements like Mg and Cu.

The heat produced during FSP might have caused segregation of Cu away from the nugget zone. The EDS detected the presence of Mg but not quantified it.

It can be revealed from Fig. 10 that the as cast structure exhibits large grains while the structure of the processed samples shows a combination of large and small grains with majority of small grains prevailing. The non-homogenous structure of the cast AA 2024/Al_2O_3 is owed to clustering of the nano particles, which are shown in Fig. 9 (d, e).

EDS pattern of those clusters confirm the presence of nano particles as shown in Fig. 10 (f). Hence, nano-Al_2O_3 particles are predispersed after FSP due to the initial clustering break, as well as to decrease amount of porosity with nano Al_2O_3 in nano-composite specimens as shown in Fig. 10 (g, h, i).

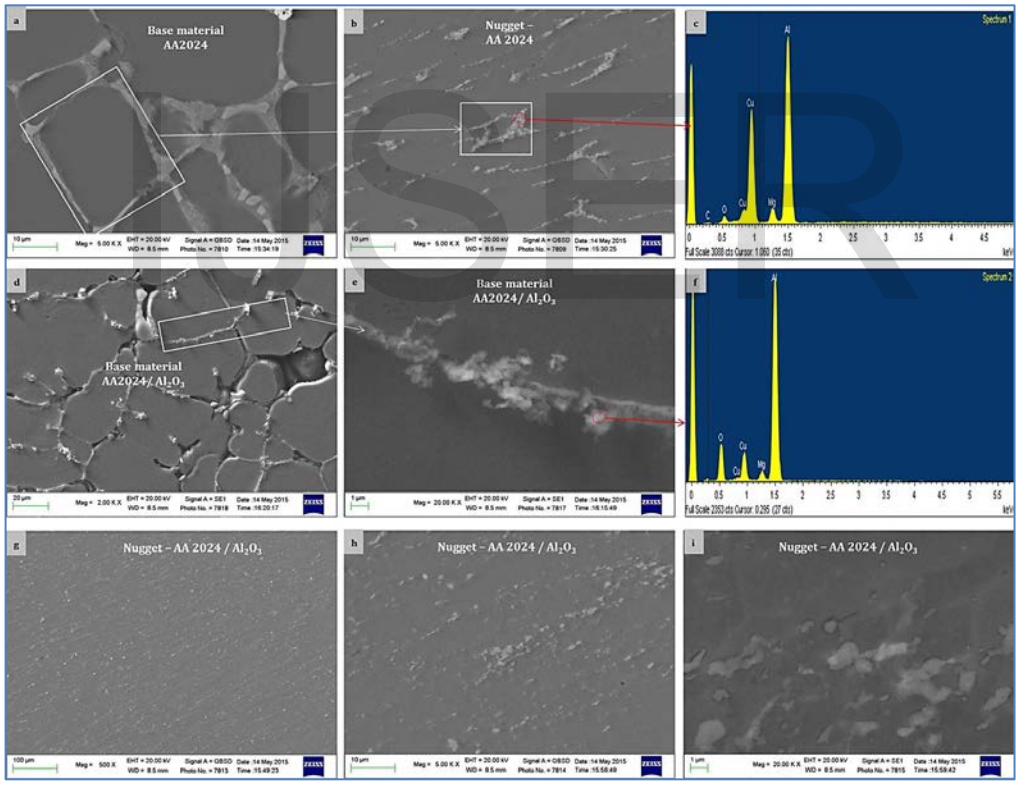

Fig.10 SEM micrographs of AA2024 base metal structure (a), compared to nugget zone structure revealed after FSP (b), accompanied with EDS analysis of the new revealed structure (c), also rheocast AA 2024/ Al_2O_3 base material at low (d) and high (e), magnification with EDS analysis (f), otherwise nugget zone structure of FSPed AA 2024/ Al_2O_3 (g, h, i), at rotation rate of 400 rpm

Similar effect was observed when 600 rpm was used as rotational speed in processing of investigated samples as shown in Fig. 10, fine nugget zone grain structure of FSPed – AA 2024.

However nanoparticles clustering were larger in size of that at 400 rpm. EDS analysis of the clusters shows that they are Al_2O_3.

Coarse grain structure was revealed at rotation speed of 800 rpm in the nugget zone compared to the grain structure revealed at rotation rates of 400 and 600 rpm. The SEM micrographs of friction stir processed rheocast AA 2024/ Al_2O_3 nugget zone, illustrates the presence of holes containing clusters as shown in Fig.12 (d), these holes were identified at high magnification as shown in Fig. 12(e). EDS analysis of the holes shows the presence of alumina particles as shown in Fig.12 (g), while analysis of the hole border illustrates the presence of intermetallic phases as shown in Fig.12 (h), this combination was not achieved in the other rotating speeds; increasing rotation speed resulted this combination.

Figure 13 shows SEM micrographs of the friction stir processed reinforced and unreinforced AA 2024 at a rotation rate of 1000 rpm.

Figure 13 (b) for the AA 2024 shows very fine globular structure in the nugget zone, similar structure is revealed on the interface of the retreating side as shown in Fig.12 (a) and advancing side as shown in Fig.13 (c).

The nugget zone of the AA 2024/ Al_2O_3 is shown to have longitudinal voids and some clusters as shown in Fig.13 (d). SEM study at higher magnification showed that these voids include huge clusters as shown in Fig.13 (e), EDEX analysis of these clusters shows the presence of alumina particles as well as a MgO phase as shown in Fig.13 (f, g). As Rhodes et al. [25] found, larger grain size, which observes in the stir zone, is occurred due to high heat input. Therefore, the refined microstructure of the surface composites is attributed to grain boundary pinning with reinforcement particles. With constant volume fraction, nanoparticles have a better distribution and therefore a growing grain boundary faces numerous obstacles in its movement. Nanoparticles and its clusters were placed along the grain boundaries and hindered grain growth. Some clustering of nanoparticles is occurred, but the percent of large clusters, in compare with clusters at 400 rpm, is too high.

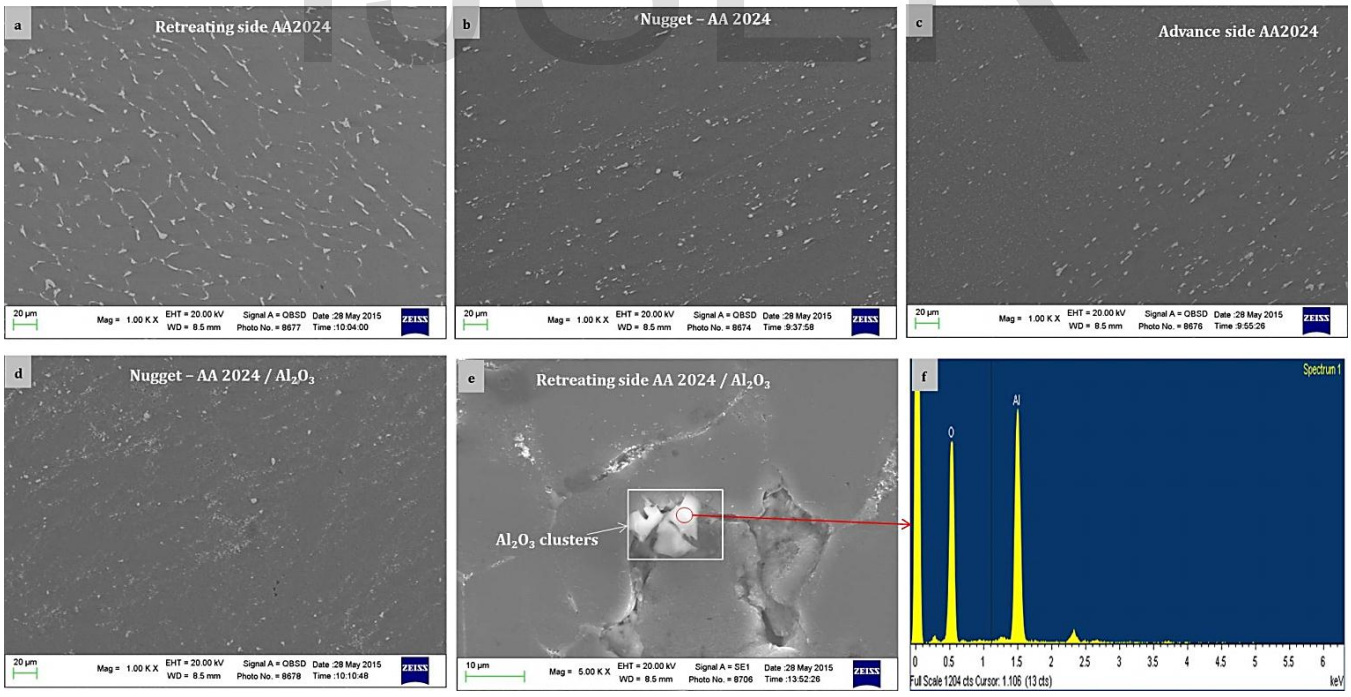

Fig.11 SEM micrographs of retreating side (a), nugget zone (b), and advance side (c) of FSPed AA 2024, and nano particles clustering and dispersion in the nugget zone at different magnifications (d ,e) accompanied with EDS analysis(f), for FSPed AA 2024/ Al_2O_3 at rotation rate of 600 rpm

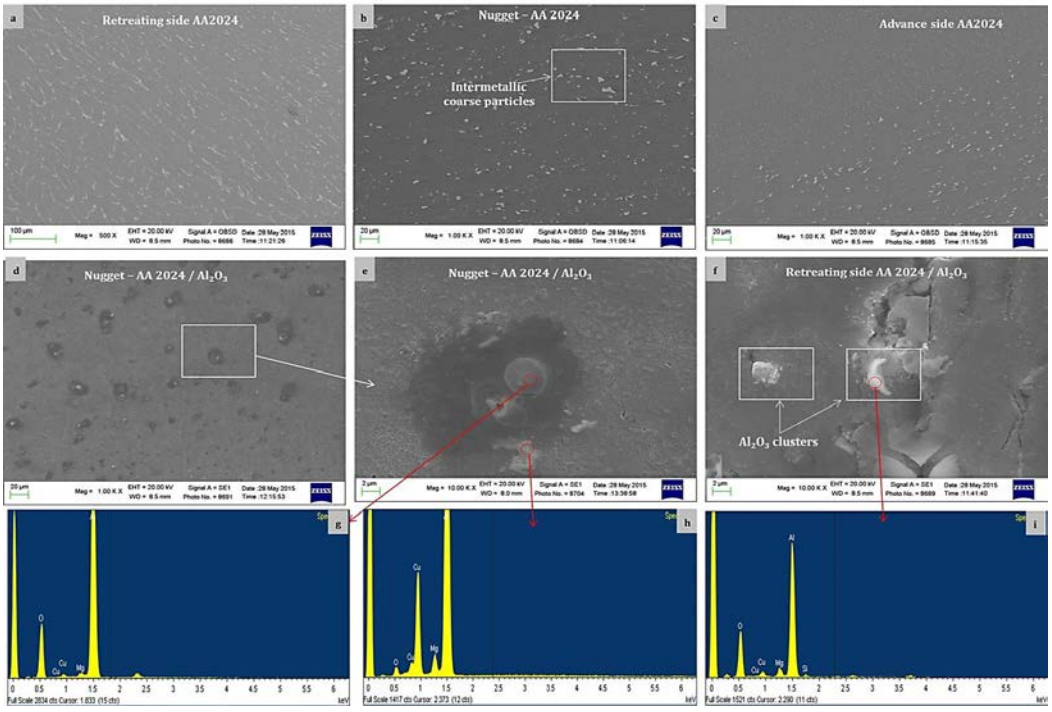

Fig.12 SEM micrographs ofretreating side (a), nugget zone (b) and advanced side (c), of processed rheocast AA 2024, also nugget zone micrograph of FSPed AA 2024/ Al_2O_3 (d),show rounded voids (e), EDS of it shows it contains alumina particles (g), and intermetallic phases on the outside border (h). Clusters on RS were found (f), EDS pattern shows presence of alumina in the clusters (i).

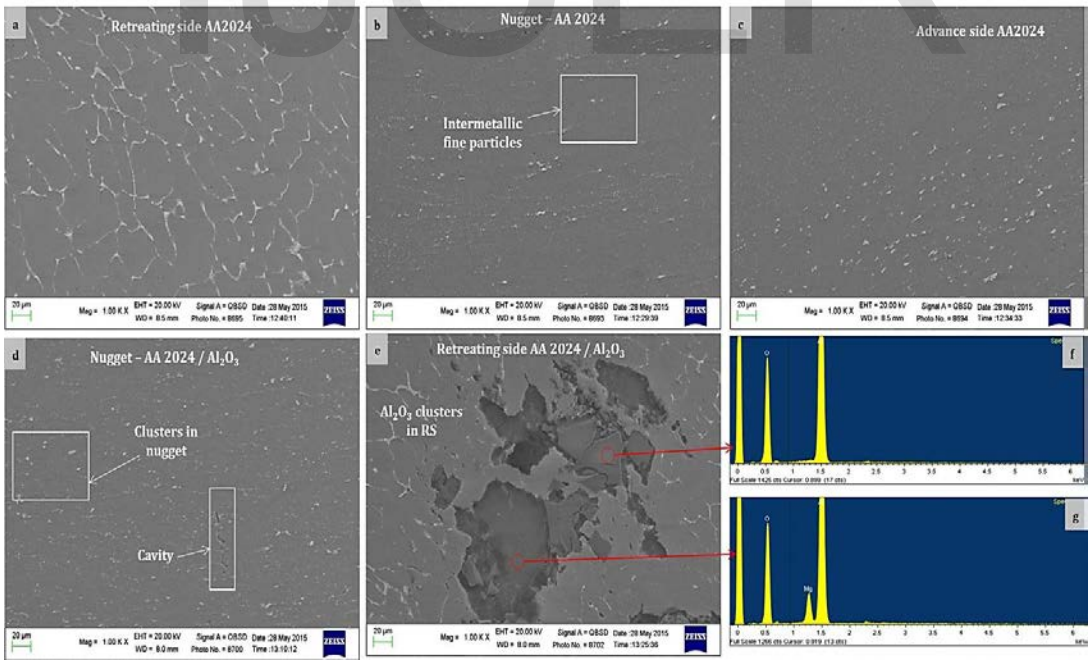

Fig.13 SEM micrographs of FSP zones; retreating side (a), nugget zone (b) and advanced side (c), of processed AA 2024, also nugget zone SEM micrograph of processed AA 2024/ Al_2O_3 showing longitudinal cavity and some clusters (d) SEM micrograph of this voids at high magnification power (e), accompanied with EDS analysis shows presence of alumina particles (f), accompanied with appearance of MgO phase, (g).

3.2 Mechanical properties

Figure14 shows typical stress- strain curves and the ultimate tensile strength values (UTS) of the cast samples before and after friction stir processing, the samples which were cast (without FSP) have an average ultimate tensile strength of43 MPa for the AA 2024 base matrix, and 72 MPa for the AA 2024 reinforced with nanoparticles.This increase of the UTS value of the nanodispersed materialis attributed to the globular grains forming during solidification, this attribution usually results from semisolid casting structure as discussed.

Significant change in the ultimate tensile strength values were observed after FSP of the samples under investigation as shown in Fig.14 (a, b).It has been also shown that the major contributions to strengthening of the composites fabricated by FSP are; 1) the fine grain size of the Al matrix resulting from the extensive plastic deformation, and 2) the Orowan strengthening due to the reinforcement particles [12]. This may suggest that the presence of nanoparticles hinders the mechanisms contributing to the conventional precipitation strengthening mechanisms in monolithic alloys. Figure 14 (d), shows the ratio of FSP sample UTS / cast samples UTS, for unreinforced and reinforced material at different rotation speeds. It is shown that the ratio of strengthening is much higher for the monolithic samples compared to the nanodispersed samples. It is also shown that the effect of FSP rotation speed on enhancing the UTS is much more significant for the monolithic alloy. For the monolithic AA 2024 increasing the rotation rate increases the UTS value more than seven times compared to the as cast samples. This may be attributed to several reasons including; the refinement of the structure and the ability to destroy the intermetallic harmful phases. As for the AA 2024 reinforced with nanoparticles, the ratio of increase in UTS resulting from FSP was only about four times at lower rpm between 400 and 800 rpm, and this ratio decreased as the rotation speed increased from 800 to 1000 rpm. This may be attributed to the effect of nanoparticles clustering.

Friction stir processing introduces a large amount of dislocations in the work piece. The rearrangement or elimination of these dislocations reduces the internal energy of the system; this is the thermodynamic driving force for recrystallization. Since aluminum has a high stacking fault energy, when the temperature is elevated, recovery occurs before recrystallization, and free dislocations rearrange themselves into subgrains surrounded by low-anglegrain boundaries; however, some dislocations remained in refined grains. The tool probe breaks most of the coarse second phases, and those fines and uniformly dispersed second phase particles have interacted with the tangled dislocations; this prohibits dislocation movement and strengthens the material during low strain deformation, which results in the increased yield stress. The increased ductility and strength observed is a result of decreasing porosity, refinement of second phases and the grain structure of the work piece [26].

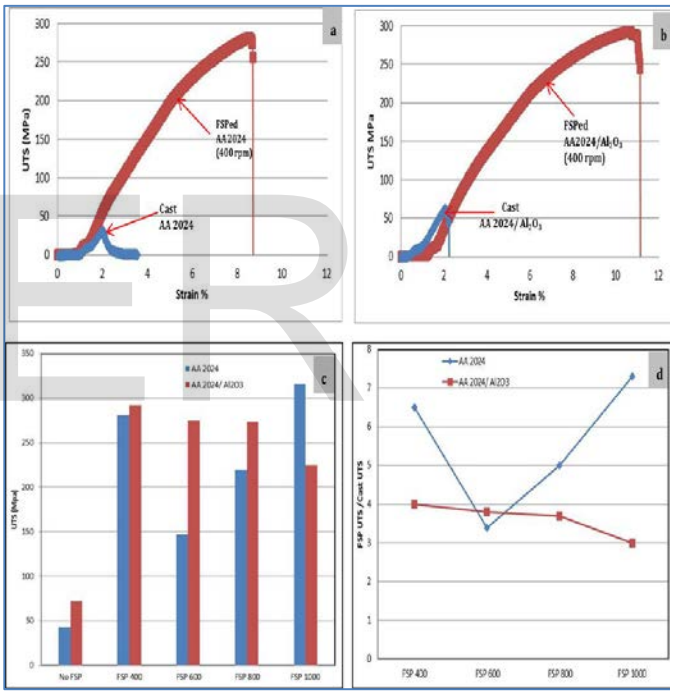

Fig.14 Stress-strain curve of AA 2024 (a) AA2024/Al_2O_3 before and after FSP at 400 rpm, UTS of AA2024 and AA2024/Al_2O_3 before and after FSP at rotation speed of 400, 600, 800 and 1000 rpm (c), ratio of FSP UTS and original UTS of cast AA 2024 and AA2024/Al_2O_3 without applying FSP.

3.2 Hardness testing

According to the well-known Hall–Petch relationship which states that the hardness is inversely proportional to grain size, after friction stir processing, remarkable increases of hardness values were recorded for matrix alloy at nugget zone with increasing rotation rate. The nano-reinforced material showed much higher hardness values across the studied profile in the nugget zone, compared to the base matrix. Surface hardening of the nanoreinforced AA2024 takes place and also higher values were noticed to be in the retreating side at low rate of rpm.

The hardness of AA 2024 and AA 2024/ Al_2O_3 cast samples without FSP, has an average value of (93 HV), and (95 HV) respectively. These values were used as a reference for comparison after applying FSP at different rotation speeds. The average hardness value of the cast nano-reinforced matrix alloy is close to that of the cast matrix alloy due to pores and cavities that formed during casting for matrix alloy and nano particles clustering for nanoreinforced matrix alloy and which was illustrated by Fig.3.

Results shows sensitive changes of hardness value due to rotation speed as shown in Figure 15, this change can be detected from hardness maps of friction stir processed cast (matrix and nanoreinforced) samples at different rotation rates of 400, 600, 800 and 1000 rpm. Hardness distribution through the thickness of the processed zone at different rotation speeds is shown in Fig.15. The highest hardness values are reported closer to the surface (at the first line which was at 0.5 mm blow the surface) for nanoreinforced matrix alloy at rotation rate of 400 rpm, the hardness value decreased as the profile hardness line is lower (far away from the surface). This increase in the hardness value of the nanoreinforced material is attributed to the homogenous dispersion of the nano particles in the nugget zone especially near surface.

The hardness variation can be explained on the basis of temperature reached at different depths. As the temperature decreases from the surface towards the bottom of the sheet, the hardness increases. Higher temperature leads to more softening and more grain growth. This result is supported by the smaller grain size at the bottom of the processed zone which was observed by Sutton et al. [27].The maximum hardness values were recorded at the center of the deformation zon (nugget).

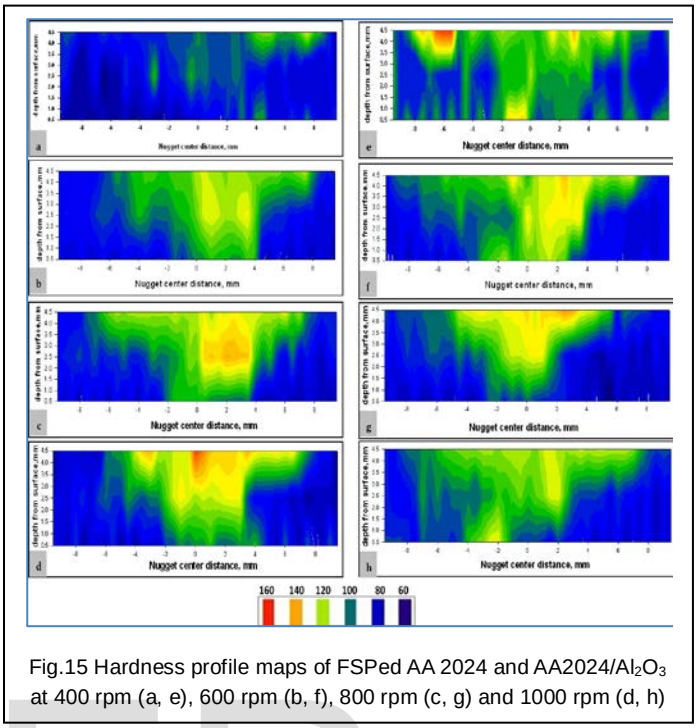

Fig.15 Hardness profile maps of FSPed AA 2024 and AA2024/Al_2O_3 at 400 rpm (a, e), 600 rpm (b, f), 800 rpm (c, g) and 1000 rpm (d, h)

An interesting result is also, illustrated in Fig. 16; for matrix, the minimum hardness values are observed at the interface between the thermo mechanical affected zone (TMAZ) and the heat affected zone (HAZ), where the hardness values are smaller than those of the base material. This was confirmed by Denquin et. al [28] and Nelsonet.al [29], the hardness drop at the heat affected zone isdue to the fact that there is no mechanical deformation (stirring) at that zone; however the peak temperature reached is enough tosoften the material near the nugget.

Nano particles used this soften regions to make it more hard but increasing FSP rotation rate does not give it chance to occupy this region so high hardness values were obtained at low rate of speeds and on same direction of rotation which is from advancing side to retreating side. These results are in agreement with the results reported by Sato et al. [30] and Darras et al.[31], on aluminum alloys. This result is expected since the temperature reached during processing increases with the rotational speed which can be achieved at lower rotational speeds. The challenge, however, is to reduce the rotational speed to allow more refinement while achieving enough heat to soften the material and allow the tool to impose large plastic deformation.That is

why it isimportant to couple the microstructure results with temperature measurements.

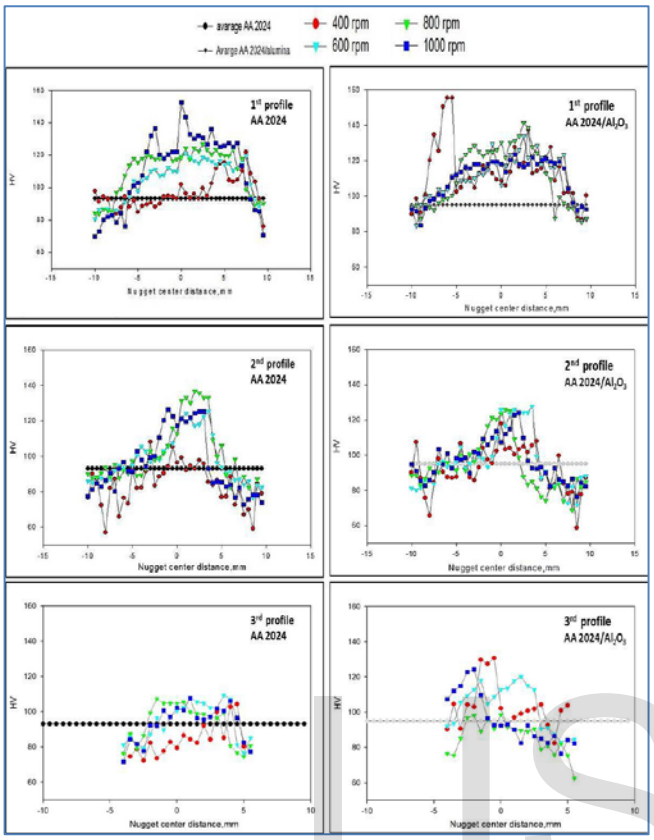

Fig.16 Hardness profiles at 0.5 mm (1st profile), 2.5 mm (2nd profile) and 4.5 mm (3rd profile) from surface of AA 2024 and AA2024/Al_2O_3

Conclusions:

In this work two routs for composite materials production have been combined to produce nanocomposite of Al_2O_3 nanoparticles in the matrix of AA2024. Nanocomposite was fabricated by casting that followed by FSP at different rotation rates. Based on this study the following conclusionscan be drawn:

- A non-uniform distribution and particle clustering of nano Al_2O_3 particulates was observed in the as cast material as well as some porosity and voids, due to casting process.
- The use of FSP greatly enhanced the distribution of the nano Al_2O_3 particles and significantly refined the grain structure of the AA2024 matrix. Furthermore, FSP eliminates the porosities and voids detected in the cast materials.
- Virtually all traces of dendritic solidification microstructure were eliminated throughout the stir zone and the intense plastic deformation and frictional heating during FSP resulted in the generation of a recrystallized fine-grained microstructure within stirred zone.
- The tensile properties of the cast monolithic AA2024 and nanocomposite is significantly enhanced after FSP. The ultimate tensile strength of the FSPed material increased to about four times, from 72 MPa for the as cast to 316 MPa after FSP.
- The hardness of the FSPed material is also significantly increased from 93 Hv for the as cast to about 155 Hv after FSP.
- Reducing the rotational speed allow more refinement while achieving enough heat to soften the material and allowthe tool to impose large plastic deformation in cast nanocomposite.

ACKNOWLEDGMENT

The authors would to thank Prof Alessandro Morri, Metallurgy group at the Department of industrial engineering, Bologna University, Italy for giving the chance to use their facilities to characterize the current materials. Also would like to thank the Ministry of scientific research Egypt for the financial support with the mobility grants no 12-12-A1 and STDF-Egypt with grant no 3926.

References

1- KamaliA. MR, Khorsand S, Amirkhanlou S, JavadN. M., "Application of compocasting and cross accumulative roll bonding processes for manufacturing high-strength, highly uniform and ultra-fine structured Al/SiCp nanocomposite," Mater Sci Eng A 592:121–127, 2014.

2- Sajjadi S, TorabiP. M, Ezatpour H, Sedghi A., "Fabrication of A356 composite reinforced with micro and nano Al_2O_3 particles by a developed compocasting method and study of its properties," J Alloys Compd 511:226–231, 2012.

3- Mazahery A., Abdizadeh H., Baharvandi H.R., "Development of high performance A356/ nano-Al_2O_3 composites," Materials Science and Engineering A, vol. 518, pp. 61–64, 2009.

4- I. El Mahallawi · Y. Shash · R. M. Rashad · M. H. Abdelaziz · J. Mayer · A. Schwed, "Hardness and wear behaviour of Semi-Solid Cast A390 Alloy Reinforced with Al2O3 and Ti-

O_2 Nanoparticles," Arab J SciEng 39:5171–5184, 2014.

5- Iman S. El-Mahallawi, Ahmed Y. S, AmerE.A., "Nanoreinforced Cast Al-Si Alloys with Al_2O_3, TiO_2 and ZrO_2 Nanoparticles," Metals (5), 802-821, 2015.

6- Hossein Z. M, Mirzaee O., Saidi P., "Structural and mechanical characterization of Al-based composite reinforced with heat treated Al_2O_3 particles," Mater Des 54:245–250, 2014.

7- Kapil K., DhirendraV., Sudhir K., "Processing and Tensile Testing of 2024 Al Matrix Composite Reinforced with Al_2O_3 Nano-Particles," 5th International &26th All India Manufacturing Technology, Design and Research Conference, India, 2014.

8- Behnam Rahimi, HamedKhosravi, Mohsen Haddad-Sabzevar, "Microstructural characteristics and mechanical properties of Al-2024 alloy processed via a rheocasting route, " International Journal of Minerals, Metallurgy and Materials Volume 22, Number 1, pp. 1, 2015.

9- C.D. Marini ,N. Fatchurrohman, "Review on the fabrication techniques of aluminium matrix nanocomposites , "Jurnal-Teknologi (Sciences & Engineering) 74:10 103–109, 2015.

10- R.S. Mishra and Z. Y. Ma, "Friction stir welding and processing", Materials Science and Engineering: R: Reports, vol. 50, no. 1-2, 1-78, 2005.

11- Pirondi, A.; Collini, L., "Analysis of crack propagation resistance of Al/Al_2O_3 particulate-reinforced composite friction stir welded butt joints", Int. J. Fatigue, 31, 111–121, 2009.

12- Shafiei-Zarghani, A., Kashani-Bozorg, S.F., Zarei-Hanzaki A., "Microstructures and mechanical properties of Al/Al_2O_3 surface nano-composite layer produced by friction stir processing", Mater.Sci. Eng., A, 500, 84–91, 2009.

13- Yong X. Gan, Daniel Solomon, Michael Reinbolt, "Friction stir Processing of particle reinforced composite materials, review", Materials, (3), 2010.

14- L Karthikeyan and V.S. Senthil Kumar, "Relationship between Process Parameters and Mechanical Properties of Friction Stir Processed M6063-T6 Aluminum Alloy", Materials and Design, Vol. 32, pp. 3085-3091, 2011.

15- T.S. Mahmoud, S.S. Mohamed, "Improvement of microstructural, mechanical characteristics of A413 cast Al Alloys using friction stir processing", Mater. Sci. Eng., A, 588, 502-509, 2012.

16- Alaa M. Hussein W., Jassim M. S., Ahmed O. Al., "Effect of friction stir processing on mechanical properties and microstructure of the cast pure aluminum", international journal of scientific & technology research, volume (2), issue 12, 2013.

17- Pirondi, A.; Collini L., "Analysis of crack propagation resistance of Al/Al_2O_3 particulate-reinforced composite friction stir welded butt joints", Int. J. Fatigue, 31, 111–121, 2009.

18- Yong X. G., Daniel S., Michael R., "Friction stir Processing of particle reinforced composite materials, review", Materials, (3), 2010.

19- M.M.Z. Ahmed, M. Refat, I. El-Mahallawi, "Manufacturing of Nano-Surface AA7075 Composites By Friction Stir Processing", Characterization of Minerals, Metals, and Materials, TMS 2014, Jon Wiley& Sons, 2014.

20- M. Refat, A.M.M. Abdelmotagaly, M.M.Z. Ahmed, I. El-Mahallawi, "The effect of heat treatment on the properties of friction stir processed AA 7075-0 with and without nano alumina additions", Friction Stir Welding and Processing VIII, TMS, 2015.

21- Marzoli L.M.,Strombeck A.V., Dos Santos J.F., Gambaro C., Volpone L. M. "Friction stir welding of an AA6061/Al2O3/20p reinforced alloy", Compos. Sci. Technol., 66, 363–371, 2006.

22- Cavaliere P. "Mechanical properties of Friction Stir Processed $2618/Al_2O_3/20p$ metal matrix composite. Composites", Part A, 36, 1657–1665, 2005.

23- M.Vykuntarao, S.ChiranjeevaRao, Ch.VinodBabu, M.V.SekharBabu "Influence of reinforced particles on the Mechanical properties ofAluminium Based Metal Matrix Composite – A Review",, ChemSci Rev Lett, 4(13), 335-341, 2015.

24- C. Leitei, R. Louro, D.M. Rodrigues "Analysis of high temperature plastic behaviour and its relation with weldability in friction stir welding for aluminium alloys AA5083-H111 and AA6082-T6" Materials and Design 37 402–409, 2012.

25- Rhodes C.G, Mahoney M. W, Bingel W. H, Calabrese M.,“Fine-grain evolution in friction-stir processed 7050 aluminum”,Scripta Mater, 48:1451–5, 2003.

26-N. Sun and D. Apelian.,“Friction Stir Processing of Aluminum Cast Alloys for High Performance Applications”, JOM , Vol. 63 No. 11 , November , 2011.

27- M. Sutton, B. Yang, A. Reynolds, R. Taylor, Microstructural studies offriction stir welds in 2024-T3 aluminum, Mater. Sci. Eng. A 323, 160–166, 2002.

28- A. Denquin, D. Allehaux, M.-H. Campaganc, G. Lapasset, Relationshipbetween microstructural variations and properties of friction stir welded6056 aluminum alloy, Weld. World, 14–19, 2002.

29- T. Nelson, R. Steel, W. Arbegast, ' In situ thermal studies and post-weldmechanical properties of friction stir welds in age hardenable aluminum', Sci. Technol. Weld. Joining 8, 283–288, 2003.

30- Y.S. Sato, M. Urata, H. Kokawa, K. Ikeda, 'Hall–Petch relationship in friction stir welds of equal channel angular-pressed aluminum alloys', Mater. Sci. Eng. A 354, 298–305, 2003.

31-B. Darras M. O., M. Khraisheh, 'Experimental thermal analysis of friction stir processing', Mater. Sci. Forum 539–543 3801–3806, 2007.